

A Measurement of the Branching Fractions of exclusive $\bar{B} \rightarrow D^{(*)}(\pi)\ell^{-}\bar{\nu}_{\ell}$ Decays in Events with a Fully Reconstructed B Meson

B. Aubert,¹ M. Bona,¹ Y. Karyotakis,¹ J. P. Lees,¹ V. Poireau,¹ X. Prudent,¹ V. Tisserand,¹ A. Zghiche,¹ J. Garra Tico,² E. Grauges,² L. Lopez,³ A. Palano,³ M. Pappagallo,³ G. Eigen,⁴ B. Stugu,⁴ L. Sun,⁴ G. S. Abrams,⁵ M. Battaglia,⁵ D. N. Brown,⁵ J. Button-Shafer,⁵ R. N. Cahn,⁵ R. G. Jacobsen,⁵ J. A. Kadyk,⁵ L. T. Kerth,⁵ Yu. G. Kolomensky,⁵ G. Kukartsev,⁵ G. Lynch,⁵ I. L. Osipenkov,⁵ M. T. Ronan,⁵ * K. Tackmann,⁵ T. Tanabe,⁵ W. A. Wenzel,⁵ P. del Amo Sanchez,⁶ C. M. Hawkes,⁶ N. Soni,⁶ A. T. Watson,⁶ H. Koch,⁷ T. Schroeder,⁷ D. Walker,⁸ D. J. Asgeirsson,⁹ T. Cuhadar-Donszelmann,⁹ B. G. Fulsom,⁹ C. Hearty,⁹ T. S. Mattison,⁹ J. A. McKenna,⁹ M. Barrett,¹⁰ A. Khan,¹⁰ M. Saleem,¹⁰ L. Teodorescu,¹⁰ V. E. Blinov,¹¹ A. D. Bukin,¹¹ A. R. Buzykaev,¹¹ V. P. Druzhinin,¹¹ V. B. Golubev,¹¹ A. P. Onuchin,¹¹ S. I. Serednyakov,¹¹ Yu. I. Skovpen,¹¹ E. P. Solodov,¹¹ K. Yu. Todyshev,¹¹ M. Bondioli,¹² S. Curry,¹² I. Eschrich,¹² D. Kirkby,¹² A. J. Lankford,¹² P. Lund,¹² M. Mandelkern,¹² E. C. Martin,¹² D. P. Stoker,¹² S. Abachi,¹³ C. Buchanan,¹³ J. W. Gary,¹⁴ F. Liu,¹⁴ O. Long,¹⁴ B. C. Shen,¹⁴ * G. M. Vitug,¹⁴ Z. Yasin,¹⁴ L. Zhang,¹⁴ H. P. Paar,¹⁵ S. Rahatlou,¹⁵ V. Sharma,¹⁵ C. Campagnari,¹⁶ T. M. Hong,¹⁶ D. Kovalskiy,¹⁶ J. D. Richman,¹⁶ T. W. Beck,¹⁷ A. M. Eisner,¹⁷ C. J. Flacco,¹⁷ C. A. Heusch,¹⁷ J. Kroseberg,¹⁷ W. S. Lockman,¹⁷ T. Schalk,¹⁷ B. A. Schumm,¹⁷ A. Seiden,¹⁷ M. G. Wilson,¹⁷ L. O. Winstrom,¹⁷ E. Chen,¹⁸ C. H. Cheng,¹⁸ D. A. Doll,¹⁸ B. Echenard,¹⁸ F. Fang,¹⁸ D. G. Hitlin,¹⁸ I. Narsky,¹⁸ T. Piatenko,¹⁸ F. C. Porter,¹⁸ R. Andreassen,¹⁹ G. Mancinelli,¹⁹ B. T. Meadows,¹⁹ K. Mishra,¹⁹ M. D. Sokoloff,¹⁹ F. Blanc,²⁰ P. C. Bloom,²⁰ W. T. Ford,²⁰ J. F. Hirschauer,²⁰ A. Kreisel,²⁰ M. Nagel,²⁰ U. Nauenberg,²⁰ A. Olivas,²⁰ J. G. Smith,²⁰ K. A. Ulmer,²⁰ S. R. Wagner,²⁰ R. Ayad,²¹ † A. M. Gabareen,²¹ A. Soffer,²¹ ‡ W. H. Toki,²¹ R. J. Wilson,²¹ D. D. Altenburg,²² E. Feltresi,²² A. Hauke,²² H. Jasper,²² M. Karbach,²² J. Merkel,²² A. Petzold,²² B. Spaan,²² K. Wacker,²² V. Klose,²³ M. J. Kobel,²³ H. M. Lacker,²³ W. F. Mader,²³ R. Nogowski,²³ J. Schubert,²³ K. R. Schubert,²³ R. Schwierz,²³ J. E. Sundermann,²³ A. Volk,²³ D. Bernard,²⁴ G. R. Bonneaud,²⁴ E. Latour,²⁴ Ch. Thiebaut,²⁴ M. Verderi,²⁴ P. J. Clark,²⁵ W. Gradl,²⁵ S. Playfer,²⁵ A. I. Robertson,²⁵ J. E. Watson,²⁵ M. Andreotti,²⁶ D. Bettoni,²⁶ C. Bozzi,²⁶ R. Calabrese,²⁶ A. Cecchi,²⁶ G. Cibinetto,²⁶ P. Franchini,²⁶ E. Luppi,²⁶ M. Negri,²⁶ A. Petrella,²⁶ L. Piemontese,²⁶ E. Prencipe,²⁶ V. Santoro,²⁶ F. Anulli,²⁷ R. Baldini-Ferrolì,²⁷ A. Calcaterra,²⁷ R. de Sangro,²⁷ G. Finocchiaro,²⁷ S. Pacetti,²⁷ P. Patteri,²⁷ I. M. Peruzzi,²⁷ § M. Piccolo,²⁷ M. Rama,²⁷ A. Zallo,²⁷ A. Buzzo,²⁸ R. Contri,²⁸ M. Lo Vetere,²⁸ M. M. Macri,²⁸ M. R. Monge,²⁸ S. Passaggio,²⁸ C. Patrignani,²⁸ E. Robutti,²⁸ A. Santroni,²⁸ S. Tosi,²⁸ K. S. Chaisanguanthum,²⁹ M. Morii,²⁹ R. S. Dubitzky,³⁰ J. Marks,³⁰ S. Schenk,³⁰ U. Uwer,³⁰ D. J. Bard,³¹ P. D. Dauncey,³¹ J. A. Nash,³¹ W. Panduro Vazquez,³¹ M. Tibbetts,³¹ P. K. Behera,³² X. Chai,³² M. J. Charles,³² U. Mallik,³² J. Cochran,³³ H. B. Crawley,³³ L. Dong,³³ V. Eyges,³³ W. T. Meyer,³³ S. Prell,³³ E. I. Rosenberg,³³ A. E. Rubin,³³ Y. Y. Gao,³⁴ A. V. Gritsan,³⁴ Z. J. Guo,³⁴ C. K. Lae,³⁴ A. G. Denig,³⁵ M. Fritsch,³⁵ G. Schott,³⁵ N. Arnaud,³⁶ J. Béquilleux,³⁶ A. D’Orazio,³⁶ M. Davier,³⁶ J. Firmino da Costa,³⁶ G. Grosdidier,³⁶ A. Höcker,³⁶ V. Lepeltier,³⁶ F. Le Diberder,³⁶ A. M. Lutz,³⁶ S. Pruvot,³⁶ P. Roudeau,³⁶ M. H. Schune,³⁶ J. Serrano,³⁶ V. Sordini,³⁶ A. Stocchi,³⁶ W. F. Wang,³⁶ G. Wormser,³⁶ D. J. Lange,³⁷ D. M. Wright,³⁷ I. Bingham,³⁸ J. P. Burke,³⁸ C. A. Chavez,³⁸ J. R. Fry,³⁸ E. Gabathuler,³⁸ R. Gamet,³⁸ D. E. Hutchcroft,³⁸ D. J. Payne,³⁸ C. Touramanis,³⁸ A. J. Bevan,³⁹ K. A. George,³⁹ F. Di Lodovico,³⁹ R. Sacco,³⁹ M. Sigamani,³⁹ G. Cowan,⁴⁰ H. U. Flaecher,⁴⁰ D. A. Hopkins,⁴⁰ S. Paramesvaran,⁴⁰ F. Salvatore,⁴⁰ A. C. Wren,⁴⁰ D. N. Brown,⁴¹ C. L. Davis,⁴¹ K. E. Alwyn,⁴² N. R. Barlow,⁴² R. J. Barlow,⁴² Y. M. Chia,⁴² C. L. Edgar,⁴² G. D. Lafferty,⁴² T. J. West,⁴² J. I. Yi,⁴² J. Anderson,⁴³ C. Chen,⁴³ A. Jawahery,⁴³ D. A. Roberts,⁴³ G. Simi,⁴³ J. M. Tuggle,⁴³ C. Dallapiccola,⁴⁴ S. S. Hertzbach,⁴⁴ X. Li,⁴⁴ E. Salvati,⁴⁴ S. Saremi,⁴⁴ R. Cowan,⁴⁵ D. Dujmic,⁴⁵ P. H. Fisher,⁴⁵ K. Koeneke,⁴⁵ G. Sciolla,⁴⁵ M. Spitznagel,⁴⁵ F. Taylor,⁴⁵ R. K. Yamamoto,⁴⁵ M. Zhao,⁴⁵ S. E. McLaughlin,⁴⁶ * P. M. Patel,⁴⁶ S. H. Robertson,⁴⁶ A. Lazzaro,⁴⁷ V. Lombardo,⁴⁷ F. Palombo,⁴⁷ J. M. Bauer,⁴⁸ L. Cremaldi,⁴⁸ V. Eschenburg,⁴⁸ R. Godang,⁴⁸ R. Kroeger,⁴⁸ D. A. Sanders,⁴⁸ D. J. Summers,⁴⁸ H. W. Zhao,⁴⁸ S. Brunet,⁴⁹ D. Côté,⁴⁹ M. Simard,⁴⁹ P. Taras,⁴⁹ F. B. Viaud,⁴⁹ H. Nicholson,⁵⁰ G. De Nardo,⁵¹ L. Lista,⁵¹ D. Monorchio,⁵¹ C. Sciacca,⁵¹ M. A. Baak,⁵² G. Raven,⁵² H. L. Snoek,⁵² C. P. Jessop,⁵³ K. J. Knoepfel,⁵³ J. M. LoSecco,⁵³ G. Benelli,⁵⁴ L. A. Corwin,⁵⁴

K. Honscheid,⁵⁴ H. Kagan,⁵⁴ R. Kass,⁵⁴ J. P. Morris,⁵⁴ A. M. Rahimi,⁵⁴ J. J. Regensburger,⁵⁴ S. J. Sekula,⁵⁴ Q. K. Wong,⁵⁴ N. L. Blount,⁵⁵ J. Brau,⁵⁵ R. Frey,⁵⁵ O. Igonkina,⁵⁵ J. A. Kolb,⁵⁵ M. Lu,⁵⁵ R. Rahmat,⁵⁵ N. B. Sinev,⁵⁵ D. Strom,⁵⁵ J. Strube,⁵⁵ E. Torrence,⁵⁵ G. Castelli,⁵⁶ N. Gagliardi,⁵⁶ A. Gaz,⁵⁶ M. Margoni,⁵⁶ M. Morandin,⁵⁶ M. Posocco,⁵⁶ M. Rotondo,⁵⁶ F. Simonetto,⁵⁶ R. Stroili,⁵⁶ C. Voci,⁵⁶ E. Ben-Haim,⁵⁷ H. Briand,⁵⁷ G. Calderini,⁵⁷ J. Chauveau,⁵⁷ P. David,⁵⁷ L. Del Buono,⁵⁷ O. Hamon,⁵⁷ Ph. Leruste,⁵⁷ J. Malclès,⁵⁷ J. Ocariz,⁵⁷ A. Perez,⁵⁷ J. Prendki,⁵⁷ L. Gladney,⁵⁸ M. Biasini,⁵⁹ R. Covarelli,⁵⁹ E. Manoni,⁵⁹ C. Angelini,⁶⁰ G. Batignani,⁶⁰ S. Bettarini,⁶⁰ M. Carpinelli,⁶⁰ A. Cervelli,⁶⁰ F. Forti,⁶⁰ M. A. Giorgi,⁶⁰ A. Lusiani,⁶⁰ G. Marchiori,⁶⁰ M. Morganti,⁶⁰ M. A. Mazur,⁶⁰ N. Neri,⁶⁰ E. Paoloni,⁶⁰ G. Rizzo,⁶⁰ J. J. Walsh,⁶⁰ J. Biesiada,⁶¹ Y. P. Lau,⁶¹ D. Lopes Pegna,⁶¹ C. Lu,⁶¹ J. Olsen,⁶¹ A. J. S. Smith,⁶¹ A. V. Telnov,⁶¹ E. Baracchini,⁶² G. Cavoto,⁶² D. del Re,⁶² E. Di Marco,⁶² R. Faccini,⁶² F. Ferrarotto,⁶² F. Ferroni,⁶² M. Gaspero,⁶² P. D. Jackson,⁶² M. A. Mazzoni,⁶² S. Morganti,⁶² G. Piredda,⁶² F. Polci,⁶² F. Renga,⁶² C. Voena,⁶² M. Ebert,⁶³ T. Hartmann,⁶³ H. Schröder,⁶³ R. Waldi,⁶³ T. Adye,⁶⁴ B. Franek,⁶⁴ E. O. Olaiya,⁶⁴ W. Roethel,⁶⁴ F. F. Wilson,⁶⁴ S. Emery,⁶⁵ M. Escalier,⁶⁵ A. Gaidot,⁶⁵ S. F. Ganzhur,⁶⁵ G. Hamel de Monchenault,⁶⁵ W. Kozanecki,⁶⁵ G. Vasseur,⁶⁵ Ch. Yèche,⁶⁵ M. Zito,⁶⁵ X. R. Chen,⁶⁶ H. Liu,⁶⁶ W. Park,⁶⁶ M. V. Purohit,⁶⁶ R. M. White,⁶⁶ J. R. Wilson,⁶⁶ M. T. Allen,⁶⁷ D. Aston,⁶⁷ R. Bartoldus,⁶⁷ P. Bechtel,⁶⁷ J. F. Benitez,⁶⁷ R. Cenci,⁶⁷ J. P. Coleman,⁶⁷ M. R. Convery,⁶⁷ J. C. Dingfelder,⁶⁷ J. Dorfan,⁶⁷ G. P. Dubois-Felsmann,⁶⁷ W. Dunwoodie,⁶⁷ R. C. Field,⁶⁷ T. Glanzman,⁶⁷ S. J. Gowdy,⁶⁷ M. T. Graham,⁶⁷ P. Grenier,⁶⁷ C. Hast,⁶⁷ W. R. Innes,⁶⁷ J. Kaminski,⁶⁷ M. H. Kelsey,⁶⁷ H. Kim,⁶⁷ P. Kim,⁶⁷ M. L. Kocian,⁶⁷ D. W. G. S. Leith,⁶⁷ S. Li,⁶⁷ B. Lindquist,⁶⁷ S. Luitz,⁶⁷ V. Luth,⁶⁷ H. L. Lynch,⁶⁷ D. B. MacFarlane,⁶⁷ H. Marsiske,⁶⁷ R. Messner,⁶⁷ D. R. Muller,⁶⁷ H. Neal,⁶⁷ S. Nelson,⁶⁷ C. P. O'Grady,⁶⁷ I. Ofte,⁶⁷ A. Perazzo,⁶⁷ M. Perl,⁶⁷ B. N. Ratcliff,⁶⁷ A. Roodman,⁶⁷ A. A. Salnikov,⁶⁷ R. H. Schindler,⁶⁷ J. Schwiening,⁶⁷ A. Snyder,⁶⁷ D. Su,⁶⁷ M. K. Sullivan,⁶⁷ K. Suzuki,⁶⁷ S. K. Swain,⁶⁷ J. M. Thompson,⁶⁷ J. Va'vra,⁶⁷ A. P. Wagner,⁶⁷ M. Weaver,⁶⁷ W. J. Wisniewski,⁶⁷ M. Wittgen,⁶⁷ D. H. Wright,⁶⁷ H. W. Wulsin,⁶⁷ A. K. Yarritu,⁶⁷ K. Yi,⁶⁷ C. C. Young,⁶⁷ V. Ziegler,⁶⁷ P. R. Burchat,⁶⁸ A. J. Edwards,⁶⁸ S. A. Majewski,⁶⁸ T. S. Miyashita,⁶⁸ B. A. Petersen,⁶⁸ L. Wilden,⁶⁸ S. Ahmed,⁶⁹ M. S. Alam,⁶⁹ R. Bula,⁶⁹ J. A. Ernst,⁶⁹ B. Pan,⁶⁹ M. A. Saeed,⁶⁹ S. B. Zain,⁶⁹ S. M. Spanier,⁷⁰ B. J. Wogslund,⁷⁰ R. Eckmann,⁷¹ J. L. Ritchie,⁷¹ A. M. Ruland,⁷¹ C. J. Schilling,⁷¹ R. F. Schwitters,⁷¹ J. M. Izen,⁷² X. C. Lou,⁷² S. Ye,⁷² F. Bianchi,⁷³ D. Gamba,⁷³ M. Pelliccioni,⁷³ M. Bomben,⁷⁴ L. Bosisio,⁷⁴ C. Cartaro,⁷⁴ F. Cossutti,⁷⁴ G. Della Ricca,⁷⁴ L. Lanceri,⁷⁴ L. Vitale,⁷⁴ V. Azzolini,⁷⁵ N. Lopez-March,⁷⁵ F. Martinez-Vidal,⁷⁵ D. A. Milanes,⁷⁵ A. Oyanguren,⁷⁵ J. Albert,⁷⁶ Sw. Banerjee,⁷⁶ B. Bhuyan,⁷⁶ K. Hamano,⁷⁶ R. Kowalewski,⁷⁶ I. M. Nugent,⁷⁶ J. M. Roney,⁷⁶ R. J. Sobie,⁷⁶ T. J. Gershon,⁷⁷ P. F. Harrison,⁷⁷ J. Ilic,⁷⁷ T. E. Latham,⁷⁷ G. B. Mohanty,⁷⁷ H. R. Band,⁷⁸ X. Chen,⁷⁸ S. Dasu,⁷⁸ K. T. Flood,⁷⁸ J. J. Hollar,⁷⁸ P. E. Kutter,⁷⁸ Y. Pan,⁷⁸ M. Pierini,⁷⁸ R. Prepost,⁷⁸ C. O. Vuosalo,⁷⁸ and S. L. Wu⁷⁸

(The BABAR Collaboration)

¹Laboratoire de Physique des Particules, IN2P3/CNRS et Université de Savoie, F-74941 Annecy-Le-Vieux, France

²Universitat de Barcelona, Facultat de Física, Departament ECM, E-08028 Barcelona, Spain

³Università di Bari, Dipartimento di Fisica and INFN, I-70126 Bari, Italy

⁴University of Bergen, Institute of Physics, N-5007 Bergen, Norway

⁵Lawrence Berkeley National Laboratory and University of California, Berkeley, California 94720, USA

⁶University of Birmingham, Birmingham, B15 2TT, United Kingdom

⁷Ruhr Universität Bochum, Institut für Experimentalphysik 1, D-44780 Bochum, Germany

⁸University of Bristol, Bristol BS8 1TL, United Kingdom

⁹University of British Columbia, Vancouver, British Columbia, Canada V6T 1Z1

¹⁰Brunel University, Uxbridge, Middlesex UB8 3PH, United Kingdom

¹¹Budker Institute of Nuclear Physics, Novosibirsk 630090, Russia

¹²University of California at Irvine, Irvine, California 92697, USA

¹³University of California at Los Angeles, Los Angeles, California 90024, USA

¹⁴University of California at Riverside, Riverside, California 92521, USA

¹⁵University of California at San Diego, La Jolla, California 92093, USA

¹⁶University of California at Santa Barbara, Santa Barbara, California 93106, USA

¹⁷University of California at Santa Cruz, Institute for Particle Physics, Santa Cruz, California 95064, USA

¹⁸California Institute of Technology, Pasadena, California 91125, USA

¹⁹University of Cincinnati, Cincinnati, Ohio 45221, USA

²⁰University of Colorado, Boulder, Colorado 80309, USA

²¹Colorado State University, Fort Collins, Colorado 80523, USA

²²Universität Dortmund, Institut für Physik, D-44221 Dortmund, Germany

²³Technische Universität Dresden, Institut für Kern- und Teilchenphysik, D-01062 Dresden, Germany

²⁴Laboratoire Leprince-Ringuet, CNRS/IN2P3, Ecole Polytechnique, F-91128 Palaiseau, France

- ²⁵ University of Edinburgh, Edinburgh EH9 3JZ, United Kingdom
- ²⁶ Università di Ferrara, Dipartimento di Fisica and INFN, I-44100 Ferrara, Italy
- ²⁷ Laboratori Nazionali di Frascati dell'INFN, I-00044 Frascati, Italy
- ²⁸ Università di Genova, Dipartimento di Fisica and INFN, I-16146 Genova, Italy
- ²⁹ Harvard University, Cambridge, Massachusetts 02138, USA
- ³⁰ Universität Heidelberg, Physikalisches Institut, Philosophenweg 12, D-69120 Heidelberg, Germany
- ³¹ Imperial College London, London, SW7 2AZ, United Kingdom
- ³² University of Iowa, Iowa City, Iowa 52242, USA
- ³³ Iowa State University, Ames, Iowa 50011-3160, USA
- ³⁴ Johns Hopkins University, Baltimore, Maryland 21218, USA
- ³⁵ Universität Karlsruhe, Institut für Experimentelle Kernphysik, D-76021 Karlsruhe, Germany
- ³⁶ Laboratoire de l'Accélérateur Linéaire, IN2P3/CNRS et Université Paris-Sud 11, Centre Scientifique d'Orsay, B. P. 34, F-91898 ORSAY Cedex, France
- ³⁷ Lawrence Livermore National Laboratory, Livermore, California 94550, USA
- ³⁸ University of Liverpool, Liverpool L69 7ZE, United Kingdom
- ³⁹ Queen Mary, University of London, E1 4NS, United Kingdom
- ⁴⁰ University of London, Royal Holloway and Bedford New College, Egham, Surrey TW20 0EX, United Kingdom
- ⁴¹ University of Louisville, Louisville, Kentucky 40292, USA
- ⁴² University of Manchester, Manchester M13 9PL, United Kingdom
- ⁴³ University of Maryland, College Park, Maryland 20742, USA
- ⁴⁴ University of Massachusetts, Amherst, Massachusetts 01003, USA
- ⁴⁵ Massachusetts Institute of Technology, Laboratory for Nuclear Science, Cambridge, Massachusetts 02139, USA
- ⁴⁶ McGill University, Montréal, Québec, Canada H3A 2T8
- ⁴⁷ Università di Milano, Dipartimento di Fisica and INFN, I-20133 Milano, Italy
- ⁴⁸ University of Mississippi, University, Mississippi 38677, USA
- ⁴⁹ Université de Montréal, Physique des Particules, Montréal, Québec, Canada H3C 3J7
- ⁵⁰ Mount Holyoke College, South Hadley, Massachusetts 01075, USA
- ⁵¹ Università di Napoli Federico II, Dipartimento di Scienze Fisiche and INFN, I-80126, Napoli, Italy
- ⁵² NIKHEF, National Institute for Nuclear Physics and High Energy Physics, NL-1009 DB Amsterdam, The Netherlands
- ⁵³ University of Notre Dame, Notre Dame, Indiana 46556, USA
- ⁵⁴ Ohio State University, Columbus, Ohio 43210, USA
- ⁵⁵ University of Oregon, Eugene, Oregon 97403, USA
- ⁵⁶ Università di Padova, Dipartimento di Fisica and INFN, I-35131 Padova, Italy
- ⁵⁷ Laboratoire de Physique Nucléaire et de Hautes Energies, IN2P3/CNRS, Université Pierre et Marie Curie-Paris6, Université Denis Diderot-Paris7, F-75252 Paris, France
- ⁵⁸ University of Pennsylvania, Philadelphia, Pennsylvania 19104, USA
- ⁵⁹ Università di Perugia, Dipartimento di Fisica and INFN, I-06100 Perugia, Italy
- ⁶⁰ Università di Pisa, Dipartimento di Fisica, Scuola Normale Superiore and INFN, I-56127 Pisa, Italy
- ⁶¹ Princeton University, Princeton, New Jersey 08544, USA
- ⁶² Università di Roma La Sapienza, Dipartimento di Fisica and INFN, I-00185 Roma, Italy
- ⁶³ Universität Rostock, D-18051 Rostock, Germany
- ⁶⁴ Rutherford Appleton Laboratory, Chilton, Didcot, Oxon, OX11 0QX, United Kingdom
- ⁶⁵ DSM/Dapnia, CEA/Saclay, F-91191 Gif-sur-Yvette, France
- ⁶⁶ University of South Carolina, Columbia, South Carolina 29208, USA
- ⁶⁷ Stanford Linear Accelerator Center, Stanford, California 94309, USA
- ⁶⁸ Stanford University, Stanford, California 94305-4060, USA
- ⁶⁹ State University of New York, Albany, New York 12222, USA
- ⁷⁰ University of Tennessee, Knoxville, Tennessee 37996, USA
- ⁷¹ University of Texas at Austin, Austin, Texas 78712, USA
- ⁷² University of Texas at Dallas, Richardson, Texas 75083, USA
- ⁷³ Università di Torino, Dipartimento di Fisica Sperimentale and INFN, I-10125 Torino, Italy
- ⁷⁴ Università di Trieste, Dipartimento di Fisica and INFN, I-34127 Trieste, Italy
- ⁷⁵ IFIC, Universitat de Valencia-CSIC, E-46071 Valencia, Spain
- ⁷⁶ University of Victoria, Victoria, British Columbia, Canada V8W 3P6
- ⁷⁷ Department of Physics, University of Warwick, Coventry CV4 7AL, United Kingdom
- ⁷⁸ University of Wisconsin, Madison, Wisconsin 53706, USA

(Dated: January 2, 2008)

We report a measurement of the branching fractions for $\bar{B} \rightarrow D^{(*)}(\pi)\ell^{-}\bar{\nu}_{\ell}$ decays based on 341.1 fb⁻¹ of data collected at the $\Upsilon(4S)$ resonance with the BABAR detector at the PEP-II $e^{+}e^{-}$ storage rings. Events are tagged by fully reconstructing one of the B mesons in a hadronic decay mode. We obtain $\mathcal{B}(B^{-} \rightarrow D^0\ell^{-}\bar{\nu}_{\ell}) = (2.33 \pm 0.09_{stat.} \pm 0.09_{syst.})\%$, $\mathcal{B}(B^{-} \rightarrow D^{*0}\ell^{-}\bar{\nu}_{\ell}) = (5.83 \pm 0.15_{stat.} \pm 0.30_{syst.})\%$, $\mathcal{B}(\bar{B}^0 \rightarrow D^{+}\ell^{-}\bar{\nu}_{\ell}) = (2.21 \pm 0.11_{stat.} \pm 0.12_{syst.})\%$, $\mathcal{B}(\bar{B}^0 \rightarrow D^{*+}\ell^{-}\bar{\nu}_{\ell}) =$

$(5.49 \pm 0.16_{stat.} \pm 0.25_{syst.})\%$, $\mathcal{B}(B^- \rightarrow D^+\pi^-\ell^-\bar{\nu}_\ell) = (0.42 \pm 0.06_{stat.} \pm 0.03_{syst.})\%$, $\mathcal{B}(B^- \rightarrow D^{*+}\pi^-\ell^-\bar{\nu}_\ell) = (0.59 \pm 0.05_{stat.} \pm 0.04_{syst.})\%$, $\mathcal{B}(\bar{B}^0 \rightarrow D^0\pi^+\ell^-\bar{\nu}_\ell) = (0.43 \pm 0.08_{stat.} \pm 0.03_{syst.})\%$ and $\mathcal{B}(\bar{B}^0 \rightarrow D^{*0}\pi^+\ell^-\bar{\nu}_\ell) = (0.48 \pm 0.08_{stat.} \pm 0.04_{syst.})\%$.

PACS numbers: 13.20He,12.38.Qk,14.40Nd

The determination of the individual exclusive branching fractions of $\bar{B} \rightarrow X_c\ell^-\bar{\nu}_\ell$ decays [1] is important for the study of the semileptonic decays of the B meson. Improvement in the knowledge of these branching fractions is also important to reduce the systematic uncertainty in the measurements of the Cabibbo-Kobayashi-Maskawa [2] matrix elements $|V_{cb}|$ and $|V_{ub}|$. For example, one of the leading sources of systematic uncertainty in the extraction of $|V_{cb}|$ from the exclusive decay $\bar{B} \rightarrow D^*\ell^-\bar{\nu}_\ell$ is the limited knowledge of the background due to $\bar{B} \rightarrow D^*\pi\ell^-\bar{\nu}_\ell$. Improved measurements of $\bar{B} \rightarrow X_c\ell^-\bar{\nu}_\ell$ decays will also benefit the accuracy of the extraction of $|V_{ub}|$, as analyses are extending into kinematic regions in which these decays represent a sizable background.

Based on current measurements [3–7] the rate of inclusive semileptonic B decays exceeds the sum of the measured exclusive decay rates [8]. While $\bar{B} \rightarrow D\ell^-\bar{\nu}_\ell$ and $D^*\ell^-\bar{\nu}_\ell$ decays account for about 70% of this total, the contribution of other states, including resonant and non-resonant $D^{(*)}\pi\ell^-\bar{\nu}_\ell$ (denoted by $D^{**}\ell^-\bar{\nu}_\ell$), is not yet well measured and may help to explain the inclusive-exclusive discrepancy.

In this letter, we present measurements of the branching fractions for $\bar{B} \rightarrow D^{(*)}(\pi)\ell^-\bar{\nu}_\ell$ decays, separately for charged and neutral B mesons.

The analysis is based on data collected with the BABAR detector [9] at the PEP-II asymmetric-energy e^+e^- storage rings. The data consist of a total of 341.1 fb^{-1} recorded at the $\Upsilon(4S)$ resonance, corresponding to 378 million $B\bar{B}$ pairs. An additional 36 fb^{-1} off-peak data sample, taken at a center-of-mass (CM) energy 40 MeV below the $\Upsilon(4S)$ resonance, is used to study background from $e^+e^- \rightarrow f\bar{f}$ ($f = u, d, s, c, \tau$) events (continuum production). A detailed GEANT4-based Monte Carlo (MC) simulation [10] of $B\bar{B}$ and continuum events is used to study the detector response, its acceptance, and to test the analysis techniques. The simulation models $\bar{B} \rightarrow D^{(*)}\ell^-\bar{\nu}_\ell$ decays using calculations based on Heavy Quark Effective Theory [11], $\bar{B} \rightarrow D^{**}(\rightarrow D^{(*)}\pi)\ell^-\bar{\nu}_\ell$ decays using the ISGW2 model [12], and $\bar{B} \rightarrow D^{(*)}\pi\ell^-\bar{\nu}_\ell$ decays using the Goity-Roberts model [13].

We select semileptonic B decays in events containing a fully reconstructed B meson (B_{tag}), which allows us to constrain the kinematics, reduce the combinatorial background, and determine the charge and flavor of the signal B meson.

We first reconstruct the semileptonic B decay, selecting a lepton with momentum p_ℓ^* in the center-of-mass frame higher than 0.6 GeV/ c . Electrons from photon conver-

sions and π^0 Dalitz decays are removed by searching for pairs of oppositely charged tracks that form a vertex with an invariant mass compatible with a photon conversion or a π^0 Dalitz decay. Candidate D^0 mesons, having the correct charge-flavor correlation with the lepton, are reconstructed in the $K^-\pi^+$, $K^-\pi^+\pi^0$, $K^-\pi^+\pi^+\pi^-$, $K_S^0\pi^+\pi^-$, $K_S^0\pi^+\pi^-\pi^0$, $K_S^0\pi^0$, K^+K^- , $\pi^+\pi^-$, and $K_S^0K_S^0$ channels, and D^+ mesons in the $K^-\pi^+\pi^+$, $K^-\pi^+\pi^+\pi^0$, $K_S^0\pi^+$, $K_S^0\pi^+\pi^0$, $K^+K^-\pi^+$, $K_S^0K^+$, and $K_S^0\pi^+\pi^+\pi^-$ channels. In events with multiple $\bar{B} \rightarrow D\ell^-\bar{\nu}_\ell$ candidates, the candidate with the best D - ℓ vertex fit is selected. Candidate D^* mesons are reconstructed by combining a D candidate with a pion or a photon in the $D^{*+} \rightarrow D^0\pi^+$, $D^{*+} \rightarrow D^+\pi^0$, $D^{*0} \rightarrow D^0\pi^0$, and $D^{*0} \rightarrow D^0\gamma$ channels. In events with multiple $\bar{B} \rightarrow D^*\ell^-\bar{\nu}_\ell$ candidates, we choose the candidate with the smallest χ^2 based on the deviations from the nominal values of the D invariant mass and the invariant mass difference between the D^* and the D , using the measured resolution.

We reconstruct B_{tag} decays of the type $\bar{B} \rightarrow DY$, where Y represents a collection of hadrons with a total charge of ± 1 , composed of $n_1\pi^\pm + n_2K^\pm + n_3K_S^0 + n_4\pi^0$, where $n_1 + n_2 \leq 5$, $n_3 \leq 2$, and $n_4 \leq 2$. Using $D^0(D^+)$ and $D^{*0}(D^{*+})$ as seeds for $B^-(\bar{B}^0)$ decays, we reconstruct about 1000 different decay chains.

The kinematic consistency of a B_{tag} candidate with a B meson decay is evaluated using two variables: the beam-energy substituted mass $m_{ES} = \sqrt{s/4 - |p_B^*|^2}$, and the energy difference $\Delta E = E_B^* - \sqrt{s}/2$. Here \sqrt{s} refers to the total CM energy, and p_B^* and E_B^* denote the momentum and energy of the B_{tag} candidate in the CM frame. For correctly identified B_{tag} decays, the m_{ES} distribution peaks at the B meson mass, while ΔE is consistent with zero. We select a B_{tag} candidate in the signal region defined as $5.27 \text{ GeV}/c^2 < m_{ES} < 5.29 \text{ GeV}/c^2$, excluding B_{tag} candidates with daughter particles in common with the charm meson or the lepton from the semileptonic B decay. In the case of multiple B_{tag} candidates in an event, we select the one with the smallest $|\Delta E|$ value. The B_{tag} and the $D^{(*)}\ell$ candidates are required to have the correct charge-flavor correlation. Mixing effects in the \bar{B}^0 sample are accounted for as described in [14]. Cross-feed effects, *i.e.*, $B_{tag}(\bar{B}_{tag}^0)$ candidates erroneously reconstructed as a neutral (charged) B , are subtracted using estimates from the simulation.

For $\bar{B} \rightarrow D^{(*)}X\ell^-\bar{\nu}_\ell$ decays, $D(D^*)$ candidates are selected within 2σ (1.5 - 2.5σ , depending on the D^* decay mode) of the D mass ($D^* - D$ mass difference), with σ typically around 8 (1-7) MeV/ c^2 . We also require the cosine of the angle between the directions of the $D^{(*)}$

candidate and the lepton in the CM frame to be less than zero, to reduce background from non- B semileptonic decays.

We reconstruct $B^- \rightarrow D^{(*)}\pi^-\ell^-\bar{\nu}_\ell$ and $\bar{B}^0 \rightarrow D^{(*)0}\pi^+\ell^-\bar{\nu}_\ell$ decays starting from the corresponding $\bar{B} \rightarrow D^{(*)}X\ell^-\bar{\nu}_\ell$ samples and selecting events with only one additional reconstructed charged track that has not been used for the reconstruction of the B_{tag} , the signal $D^{(*)}$, or the lepton. For the $\bar{B}^0 \rightarrow D^0\pi^+\ell^-\bar{\nu}_\ell$ and the $\bar{B}^0 \rightarrow D^{*0}\pi^+\ell^-\bar{\nu}_\ell$ decays, we additionally require the invariant mass difference $M(D\pi) - M(D)$ to be greater than $0.18 \text{ GeV}/c^2$ to veto $\bar{B}^0 \rightarrow D^{*+}\ell^-\bar{\nu}_\ell$ events. To reduce the combinatorial background in the $\bar{B}^0 \rightarrow D^{*0}\pi^+\ell^-\bar{\nu}_\ell$ mode, we also require the total extra energy in the event, obtained by summing the energy of all the showers in the electromagnetic calorimeter that have not been assigned to the B_{tag} or the $D^{(*)}\ell^-$ candidates, to be less than 1 GeV .

The exclusive semileptonic B decays are identified by the missing mass squared in the event, $m_{miss}^2 = (p(\Upsilon(4S)) - p(B_{tag}) - p(D^{(*)}(\pi)) - p(\ell))^2$, defined in terms of the particle four-momenta in the CM frame of the reconstructed final states. For correctly reconstructed signal events, the only missing particle is the neutrino, and m_{miss}^2 peaks at zero. Other B semileptonic decays, where one particle is not reconstructed (feed-down) or is erroneously added (feed-up) to the charm candidate, exhibit higher or lower values in m_{miss}^2 . To obtain the B semileptonic signal yields, we perform a one-dimensional extended binned maximum likelihood fit [15] to the m_{miss}^2 distributions. The fitted data samples are assumed to contain four different types of events: $\bar{B} \rightarrow D^{(*)}(\pi)\ell^-\bar{\nu}_\ell$ signal events, feed-down or feed-up from other B semileptonic decays, combinatoric $B\bar{B}$ and continuum background, and hadronic B decays (mainly due to hadrons misidentified as leptons). For the fit to the m_{miss}^2 distributions of the $\bar{B} \rightarrow D^{(*)}\pi\ell^-\bar{\nu}_\ell$ channel, we also include a component corresponding to other misreconstructed $\bar{B} \rightarrow D^{**}(D^*\pi)\ell^-\bar{\nu}_\ell$ decays. We use the MC predictions for the different B semileptonic decay m_{miss}^2 distributions to obtain the Probability Density Functions (PDFs). The combinatoric $B\bar{B}$ and continuum background shape is also estimated by the MC simulation, and we use the off-peak data to provide the continuum background normalization. The shape of the continuum background distribution predicted by the MC simulation is consistent with that obtained from the off-peak data.

The m_{miss}^2 distributions are compared with the results of the fits in Fig. 1 for each of the $\bar{B} \rightarrow D^{(*)}(\pi)\ell^-\bar{\nu}_\ell$ channels. The fitted signal yields and the signal efficiencies, accounting for the B_{tag} reconstruction, are listed in Table I.

To reduce the systematic uncertainty, the exclusive $\mathcal{B}(\bar{B} \rightarrow D^{(*)}(\pi)\ell^-\bar{\nu}_\ell)$ branching fractions relative to the inclusive semileptonic fraction are measured. A sample of $\bar{B} \rightarrow X\ell^-\bar{\nu}_\ell$ events is selected by identifying

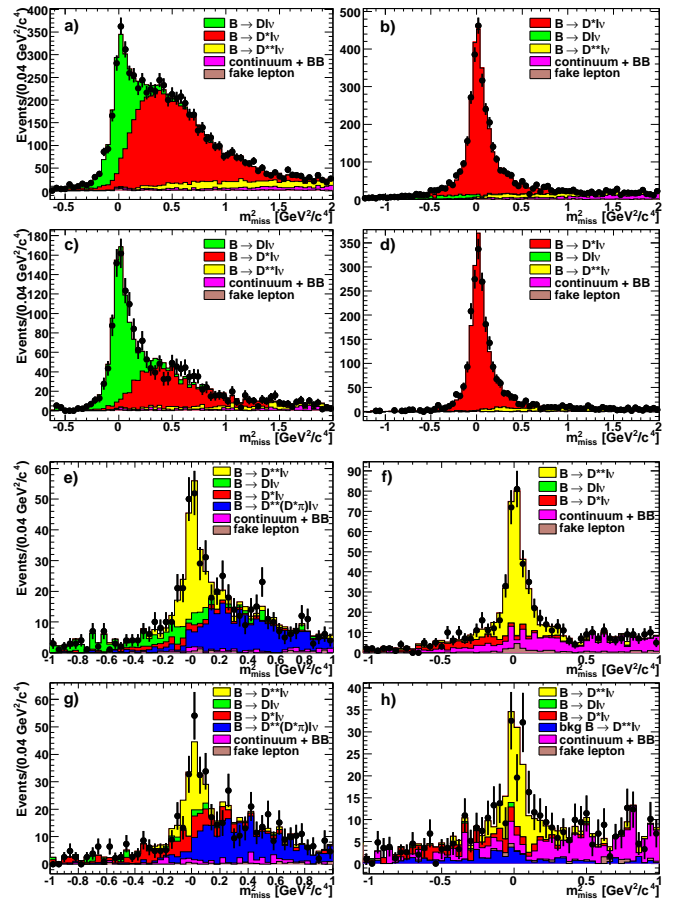


FIG. 1: (Color online) Fit to the m_{miss}^2 distribution for a) $B^- \rightarrow D^0\ell^-\bar{\nu}_\ell$, b) $B^- \rightarrow D^{*0}\ell^-\bar{\nu}_\ell$, c) $\bar{B}^0 \rightarrow D^+\ell^-\bar{\nu}_\ell$, d) $\bar{B}^0 \rightarrow D^{*+}\ell^-\bar{\nu}_\ell$, e) $B^- \rightarrow D^+\pi^-\ell^-\bar{\nu}_\ell$, f) $B^- \rightarrow D^{*+}\pi^-\ell^-\bar{\nu}_\ell$, g) $\bar{B}^0 \rightarrow D^0\pi^+\ell^-\bar{\nu}_\ell$, and h) $\bar{B}^0 \rightarrow D^{*0}\pi^+\ell^-\bar{\nu}_\ell$; the data (points with error bars) are compared to the results of the overall fit (sum of the solid histograms). The PDFs for the different fit components are stacked and shown in different colors.

a charged lepton with CM momentum greater than $0.6 \text{ GeV}/c$ and the correct charge-flavor correlation with the B_{tag} candidate. In the case of multiple B_{tag} candidates in an event, we select the one reconstructed in the decay channel with the highest purity, defined as the fraction of signal events in the m_{ES} signal region. Background components peaking in the m_{ES} signal region include cascade B meson decays (*i.e.*, the lepton does not come directly from the B) and hadronic decays, and are subtracted by using the corresponding MC distributions. The total yield for the inclusive $\bar{B} \rightarrow X\ell^-\bar{\nu}_\ell$ decays is obtained from a maximum likelihood fit to the m_{ES} distribution of the B_{tag} candidates using an ARGUS function [16] for the description of the combinatorial $B\bar{B}$ and continuum background, and a Crystal Ball function [17] for the signal. Additional Crystal Ball and ARGUS functions are used to model a broad-peaking component, included

in the signal definition, due to real $\bar{B} \rightarrow X\ell^-\bar{\nu}_\ell$ decays for which, in the B_{tag} reconstruction, neutral particles have not been identified or have been interchanged with the semileptonic decays. Fig. 2 shows the m_{ES} distribution of the B_{tag} candidates in the $B^- \rightarrow X\ell^-\bar{\nu}_\ell$ and $\bar{B}^0 \rightarrow X\ell^-\bar{\nu}_\ell$ sample. The fit yields 159896 ± 1361 events for the $B^- \rightarrow X\ell^-\bar{\nu}_\ell$ sample and 96771 ± 968 events for the $\bar{B}^0 \rightarrow X\ell^-\bar{\nu}_\ell$ sample.

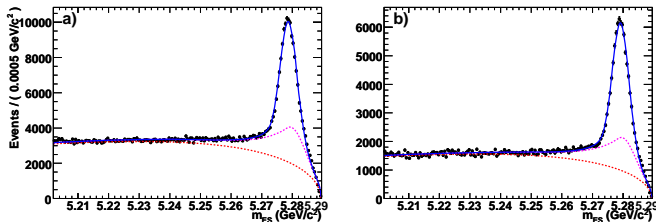


FIG. 2: (Color online) m_{ES} distributions of the a) $B^- \rightarrow X\ell^-\bar{\nu}_\ell$, and b) $\bar{B}^0 \rightarrow X\ell^-\bar{\nu}_\ell$ samples. The data (points with error bars) are compared to the result of the fit (solid line). The dashed lines show the broad-peaking component and the sum of the combinatorial and continuum background.

The relative branching fractions $\mathcal{B}(\bar{B} \rightarrow D^{(*)}(\pi)\ell^-\bar{\nu}_\ell)/\mathcal{B}(\bar{B} \rightarrow X\ell^-\bar{\nu}_\ell)$ are obtained by correcting the signal yields for the reconstruction efficiencies (estimated from $B\bar{B}$ MC events) and normalizing to the inclusive $\bar{B} \rightarrow X\ell^-\bar{\nu}_\ell$ signal yield, following the relation $\mathcal{B}(\bar{B} \rightarrow D^{(*)}(\pi)\ell^-\bar{\nu}_\ell)/\mathcal{B}(\bar{B} \rightarrow X\ell^-\bar{\nu}_\ell) = \frac{N_{sig}}{\epsilon_{sig}} \frac{\epsilon_{sl}}{N_{sl}}$. Here, N_{sig} is the number of $\bar{B} \rightarrow D^{(*)}(\pi)\ell^-\bar{\nu}_\ell$ signal events for the various modes, reported in Table I together with the corresponding reconstruction efficiencies ϵ_{sig} , N_{sl} is the $\bar{B} \rightarrow X\ell^-\bar{\nu}_\ell$ signal yield, and ϵ_{sl} is the corresponding reconstruction efficiency including the B_{tag} reconstruction, equal to 0.36% and 0.23% for the $B^- \rightarrow X\ell^-\bar{\nu}_\ell$ and $\bar{B}^0 \rightarrow X\ell^-\bar{\nu}_\ell$ decays, respectively. The absolute branching fractions $\mathcal{B}(\bar{B} \rightarrow D^{(*)}(\pi)\ell^-\bar{\nu}_\ell)$ are then determined using the semileptonic branching fraction $\mathcal{B}(\bar{B} \rightarrow X\ell^-\bar{\nu}_\ell) = (10.78 \pm 0.18)\%$ and the ratio of the B^0 and the B^+ lifetimes $\tau_{B^+}/\tau_{B^0} = 1.071 \pm 0.009$ [8].

Numerous sources of systematic uncertainties have been investigated. The uncertainties due to the detector simulation are established by varying, within bounds given by data control samples, the tracking efficiency of all charged tracks (resulting in 1.2-2.7% relative systematic uncertainty among the different decay modes), the calorimeter efficiency (0.5-1.8%), the lepton identification efficiency (0.4-3%), and the reconstruction efficiency for low momentum charged (1.2%) and neutral pions (1.3%). We evaluate the systematic uncertainties associated with the MC simulation of various signal and background processes: photon conversion and π^0 Dalitz decay (0.04-0.4%), B cascade decay contamination (0.6-1%), and flavor cross-feed (0.2-0.3%). We vary the $\bar{B} \rightarrow D\ell^-\bar{\nu}_\ell$ and $\bar{B} \rightarrow D^*\ell^-\bar{\nu}_\ell$ form factors within their measured uncertainties [11] (0.4-0.8%) and we include the uncertainty on

the branching fractions of the reconstructed D and D^* modes (2.3-4.4%), and on the absolute branching fraction $\mathcal{B}(\bar{B} \rightarrow X\ell^-\bar{\nu}_\ell)$ used for the normalization (1.9%). We also include a systematic uncertainty due to differences in the efficiency of the B_{tag} selection in the exclusive selection of $\bar{B} \rightarrow D^{(*)}(\pi)\ell^-\bar{\nu}_\ell$ decays and the inclusive $\bar{B} \rightarrow X\ell^-\bar{\nu}_\ell$ reconstruction (0.9-5.6%), and the extraction of the $\bar{B} \rightarrow D^{(*)}(\pi)\ell^-\bar{\nu}_\ell$ (0.4-1.8%) and $\bar{B} \rightarrow X\ell^-\bar{\nu}_\ell$ (0.5-0.9%) signal yields. The complete set of systematic uncertainties is given in Ref. [18].

We measure the following branching fractions:

$$\begin{aligned} \mathcal{B}(B^- \rightarrow D^0\ell^-\bar{\nu}_\ell) &= (2.33 \pm 0.09_{stat.} \pm 0.09_{syst.})\% \\ \mathcal{B}(B^- \rightarrow D^{*0}\ell^-\bar{\nu}_\ell) &= (5.83 \pm 0.15_{stat.} \pm 0.30_{syst.})\% \\ \mathcal{B}(\bar{B}^0 \rightarrow D^+\ell^-\bar{\nu}_\ell) &= (2.21 \pm 0.11_{stat.} \pm 0.12_{syst.})\% \\ \mathcal{B}(\bar{B}^0 \rightarrow D^{*+}\ell^-\bar{\nu}_\ell) &= (5.49 \pm 0.16_{stat.} \pm 0.25_{syst.})\% \\ \mathcal{B}(B^- \rightarrow D^+\pi^-\ell^-\bar{\nu}_\ell) &= (0.42 \pm 0.06_{stat.} \pm 0.03_{syst.})\% \\ \mathcal{B}(B^- \rightarrow D^{*+}\pi^-\ell^-\bar{\nu}_\ell) &= (0.59 \pm 0.05_{stat.} \pm 0.04_{syst.})\% \\ \mathcal{B}(\bar{B}^0 \rightarrow D^0\pi^+\ell^-\bar{\nu}_\ell) &= (0.43 \pm 0.08_{stat.} \pm 0.03_{syst.})\% \\ \mathcal{B}(\bar{B}^0 \rightarrow D^{*0}\pi^+\ell^-\bar{\nu}_\ell) &= (0.48 \pm 0.08_{stat.} \pm 0.04_{syst.})\%. \end{aligned}$$

The accuracy of the branching fraction measurements for the $\bar{B} \rightarrow D^{(*)}\ell^-\bar{\nu}_\ell$ decays is comparable to that of the current world average [8]. We compute the total branching fractions of the $\bar{B} \rightarrow D^{(*)}\pi\ell^-\bar{\nu}_\ell$ decays assuming isospin symmetry, $\mathcal{B}(\bar{B} \rightarrow D^{(*)}\pi\ell^-\bar{\nu}_\ell) = \frac{1}{2}\mathcal{B}(\bar{B} \rightarrow D^{(*)}\pi^\pm\ell^-\bar{\nu}_\ell)$, to estimate the branching fractions of $D^{(*)}\pi^0$ final states, obtaining:

$$\begin{aligned} \mathcal{B}(B^- \rightarrow D^{(*)}\pi\ell^-\bar{\nu}_\ell) &= (1.52 \pm 0.12_{stat.} \pm 0.10_{syst.})\% \\ \mathcal{B}(\bar{B}^0 \rightarrow D^{(*)}\pi\ell^-\bar{\nu}_\ell) &= (1.37 \pm 0.17_{stat.} \pm 0.10_{syst.})\%, \end{aligned}$$

where we assume the systematic uncertainties on the $\bar{B} \rightarrow D\pi\ell^-\bar{\nu}_\ell$ and $\bar{B} \rightarrow D^*\pi\ell^-\bar{\nu}_\ell$ modes to be completely correlated. These results are consistent with, but have smaller uncertainties than, recent results from the Belle collaboration [7].

By comparing the sum of the measured branching fractions for $\bar{B} \rightarrow D^{(*)}(\pi)\ell^-\bar{\nu}_\ell$ with the inclusive $\bar{B} \rightarrow X_c\ell^-\bar{\nu}_\ell$ branching fraction [8], a $(11 \pm 4)\%$ discrepancy is observed, which is most likely due to $\bar{B} \rightarrow D^{(*)}n\pi\ell^-\bar{\nu}_\ell$ decays with $n > 1$.

We are grateful for the excellent luminosity and machine conditions provided by our PEP-II colleagues, and for the substantial dedicated effort from the computing organizations that support BABAR. The collaborating institutions wish to thank SLAC for its support and kind hospitality. This work is supported by DOE and NSF (USA), NSERC (Canada), CEA and CNRS-IN2P3 (France), BMBF and DFG (Germany), INFN (Italy),

TABLE I: Signal yields and reconstruction efficiencies for the $\bar{B} \rightarrow D^{(*)}(\pi)\ell^{-}\bar{\nu}_{\ell}$ decays.

Decay Mode	N_{sig}	$\epsilon_{sig}(\times 10^{-4})$	Decay Mode	N_{sig}	$\epsilon_{sig}(\times 10^{-4})$
$B^{-} \rightarrow D^0\ell^{-}\bar{\nu}_{\ell}$	1635 ± 61	1.71 ± 0.02	$B^{-} \rightarrow D^{+}\pi^{-}\ell^{-}\bar{\nu}_{\ell}$	174 ± 25	1.02 ± 0.03
$B^{-} \rightarrow D^{*0}\ell^{-}\bar{\nu}_{\ell}$	3050 ± 73	1.27 ± 0.01	$B^{-} \rightarrow D^{*+}\pi^{-}\ell^{-}\bar{\nu}_{\ell}$	306 ± 27	1.26 ± 0.03
$\bar{B}^0 \rightarrow D^{+}\ell^{-}\bar{\nu}_{\ell}$	852 ± 40	0.94 ± 0.02	$\bar{B}^0 \rightarrow D^0\pi^{+}\ell^{-}\bar{\nu}_{\ell}$	107 ± 20	0.60 ± 0.03
$\bar{B}^0 \rightarrow D^{*+}\ell^{-}\bar{\nu}_{\ell}$	2045 ± 55	0.91 ± 0.01	$\bar{B}^0 \rightarrow D^{*0}\pi^{+}\ell^{-}\bar{\nu}_{\ell}$	130 ± 20	0.66 ± 0.02

FOM (The Netherlands), NFR (Norway), MIST (Russia), MEC (Spain), and STFC (United Kingdom). Individuals have received support from the Marie Curie EIF (European Union) and the A. P. Sloan Foundation.

of systematic uncertainties. For more information on EPAPS, see <http://www.aip.org/pubservs/epaps.html>.

* Deceased

† Now at Temple University, Philadelphia, Pennsylvania 19122, USA

‡ Now at Tel Aviv University, Tel Aviv, 69978, Israel

§ Also with Università di Perugia, Dipartimento di Fisica, Perugia, Italy

¶ Also with Università di Sassari, Sassari, Italy

- [1] Here X_c refers to any charm hadronic state, X_u to any charmless hadronic state, $X = X_c + X_u$ and $\ell = e, \mu$. The charge conjugate state is always implied unless stated otherwise.
- [2] M. Kobayashi and T. Maskawa, Prog. Theor. Phys. **49**, 652 (1973).
- [3] D. Buskulic *et al.* (ALEPH Collab.), Z. Phys. C **73**, 601 (1997).
- [4] P. Abreu *et al.* (DELPHI Collab.), Phys. Lett. B **475**, 407 (2000).
- [5] B. Aubert *et al.* (BABAR Collab.), Phys. Rev. D **71**, 051502 (2005).
- [6] B. Aubert *et al.* (BABAR Collab.), Phys. Rev. D **76**, 051101 (2007).
- [7] D. Liventsev *et al.* (Belle Collab.), Phys. Rev. D **72**, 051109 (2005).
- [8] W.-M. Yao *et al.* (Particle Data Group), J. Phys. G **33**, 1 (2006).
- [9] B. Aubert *et al.* (BABAR Collab.), Nucl. Instrum. Methods A **479**, 1 (2002).
- [10] S. Agostinelli *et al.*, Nucl. Instrum. Methods A **506**, 250 (2003).
- [11] I. Caprini, L. Lellouch and M. Neubert, Nucl. Phys. B **505**, 65 (1997); B. Aubert *et al.* (BABAR Collaboration), arXiv:0705.4008 [hep-ex], submitted to PRD.
- [12] D. Scora and N. Isgur, Phys. Rev. D **52**, 2783 (1995). See also N. Isgur *et al.*, Phys. Rev. D **39**, 799 (1989).
- [13] L. Goity and W. Roberts, Phys. Rev. D **51**, 3459 (1995).
- [14] B. Aubert *et al.* (BABAR Collaboration), Phys. Rev. D **69**, 111104 (2004).
- [15] R. J. Barlow and C. Beeston, Comput. Phys. Commun. **77**, 219 (1993).
- [16] H. Albrecht *et al.* (ARGUS Collaboration), Z. Phys. C **48**, 543 (1990).
- [17] M. J. Oreglia, SLAC-236 (1980); J. E. Gaiser, SLAC-255 (1982); T. Skwarnicki, DESY F31-86-02 (1986).
- [18] See EPAPS Document No. *xxxxx* for the complete set

Electronic Physics Auxiliary Publication Service (EPAPS)

This is an EPAPS attachment to B. Aubert *et al.* (BABAR Collaboration), BABAR-PUB-07/071, SLAC-PUB-13056, arXiv:0712.3503 [hep-ex], submitted to Phys. Rev. Lett. For more information on EPAPS, see <http://www.aip.org/pubservs/epaps.html>.

TABLE II: Systematic uncertainties (relative errors in %) in the measurement of $\mathcal{B}(\bar{B} \rightarrow D^{(*)}\ell^-\bar{\nu}_\ell)/\mathcal{B}(\bar{B} \rightarrow X\ell^-\bar{\nu}_\ell)$.

	Systematic uncertainty on $\mathcal{B}(\bar{B} \rightarrow D^{(*)}\ell^-\bar{\nu}_\ell)/\mathcal{B}(\bar{B} \rightarrow X\ell^-\bar{\nu}_\ell)$			
	$B^- \rightarrow D^0\ell^-\bar{\nu}_\ell$	$B^- \rightarrow D^{*0}\ell^-\bar{\nu}_\ell$	$B^0 \rightarrow D^+\ell^-\bar{\nu}_\ell$	$B^0 \rightarrow D^{*+}\ell^-\bar{\nu}_\ell$
Tracking efficiency	1.4	1.2	1.4	1.5
Neutral reconstruction lepton ID	0.7	1.9	0.5	1.1
Soft particle efficiency	0.5	0.4	0.5	0.6
Monte Carlo corrections	-	1.3	-	1.2
Conversion and Dalitz decay background	0.04	0.07	0.06	0.05
Cascade $\bar{B} \rightarrow X \rightarrow \ell^-$ decay background	0.6	0.6	1.0	1.0
$\bar{B}^0 - B^-$ cross-feed	0.2	0.3	0.2	0.3
Form factors	0.4	0.8	0.4	0.8
D branching fractions	2.3	2.1	4.1	2.6
D^* branching fractions	-	2.8	-	0.8
$\bar{B} \rightarrow X\ell^-\bar{\nu}_\ell$ branching fraction	1.9	1.9	1.9	1.9
B_{tag} selection	0.9	1.7	1.8	1.3
Fit technique				
$\bar{B} \rightarrow X\ell^-\bar{\nu}_\ell$ yield	0.5	0.5	0.9	0.9
$\bar{B} \rightarrow D^{(*)}\ell^-\bar{\nu}_\ell$ yield	0.6	0.4	1.2	0.4
Total systematic error	3.7	5.2	5.4	4.5

TABLE III: Systematic uncertainties (relative errors in %) in the measurement of $\mathcal{B}(\bar{B} \rightarrow D^{(*)}\pi\ell^-\bar{\nu}_\ell)/\mathcal{B}(\bar{B} \rightarrow X\ell^-\bar{\nu}_\ell)$.

	Systematic uncertainty on $\mathcal{B}(\bar{B} \rightarrow D^{(*)}\pi\ell^-\bar{\nu}_\ell)/\mathcal{B}(\bar{B} \rightarrow X\ell^-\bar{\nu}_\ell)$			
	$B^- \rightarrow D^+\pi^-\ell^-\bar{\nu}_\ell$	$B^- \rightarrow D^{*+}\pi^-\ell^-\bar{\nu}_\ell$	$B^0 \rightarrow D^0\pi^+\ell^-\bar{\nu}_\ell$	$B^0 \rightarrow D^{*0}\pi^+\ell^-\bar{\nu}_\ell$
Tracking efficiency	1.8	2.7	1.5	1.7
Neutral reconstruction lepton ID	1.7	1.8	1.1	1.8
Soft particle efficiency	2.3	3.0	2.6	1.8
Monte Carlo corrections	-	1.2	-	1.3
Conversion and Dalitz decay background	0.15	0.4	0.05	0.2
Cascade $\bar{B} \rightarrow X \rightarrow \ell^-$ decay background	0.6	0.6	1.0	1.0
$\bar{B}^0 - B^-$ cross-feed	0.2	0.3	0.2	0.3
Form factors	0.4	0.8	0.4	0.8
D branching fractions	4.2	2.8	2.5	2.9
D^* branching fractions	-	0.9	-	3.3
$\bar{B} \rightarrow X\ell^-\bar{\nu}_\ell$ branching fraction	1.9	1.9	1.9	1.9
B_{tag} selection	5.0	4.3	4.0	5.6
Fit technique				
$\bar{B} \rightarrow X\ell^-\bar{\nu}_\ell$ yield	0.5	0.5	0.9	0.9
$\bar{B} \rightarrow D^{(*)}\pi\ell^-\bar{\nu}_\ell$ yield	1.2	0.9	1.8	1.5
Total systematic error	7.7	7.3	6.4	8.4